ACCOUNTS of chemical research

pubs.acs.org/accounts Article

Investigation of Active Catalysts at Work

Irene M. N. Groot*

Cite This: *Acc. Chem. Res.* 2021, 54, 4334−4341 Read Online

ACCESS | Metrics & More | Article Recommendations

CONSPECTUS: Even after being in business for at least the last 100 years, research into the field of (heterogeneous) catalysis is still vibrant, both in academia and in industry. One of the reasons for this is that around 90% of all chemicals and materials used in everyday life are produced employing catalysis. In 2020, the global catalyst market size reached $35 billion, and it is still steadily increasing every year. Additionally, catalysts will be the driving force behind the transition toward sustainable energy. However, even after having been investigated for 100 years, we still have not reached the holy grail of developing catalysts from rational design instead of from trial-and-error. There are two main reasons for this, indicated by the two so-called "gaps" between (academic) research and actual catalysis. The first one is the "pressure gap", indicating the 13 orders of magnitude difference in pressure between the ultrahigh vacuum lab conditions and the atmospheric pressures (and higher) of industrial catalysis. The second one is the "materials gap", indicating the difference in complexity between single-crystal model catalysts of academic research and the real catalysts, consisting of metallic nanoparticles on supports, promoters, fillers, and binders. Although over the past decades significant efforts have been made in closing these gaps, many steps still have to be taken. In this Account, I will discuss the steps we have taken at Leiden University to further our fundamental understanding of heterogeneous catalysis at the (near-)atomic scale. I will focus on bridging the pressure gap, though we are also working on closing the materials gap. Over the past years, we developed state-of-the-art equipment that is able to investigate the (near-)atomic-scale structure of the catalyst surface during the chemical reaction using several surface-science-based techniques such as scanning tunneling microscopy, atomic force microscopy, optical microscopy, and X-ray-based techniques (surface X-ray diffraction, grazing-incidence small-angle X-ray scattering, and X-ray reflectivity, in collaboration with ESRF). Simultaneously with imaging the surface, we can investigate the catalyst's performance via mass spectrometry, enabling us to link changes in the catalyst structure to its activity, selectivity, or stability. Although we are currently investigating many industrially relevant catalytic systems, I will here focus the discussion on the oxidation of platinum during, for example, CO and NO oxidation, the NO reduction reaction on platinum, and the growth of graphene on liquid (molten) copper. I will show that to be able to obtain the full picture of heterogeneous catalysis, the ability to investigate the catalyst at the (near-)atomic scale *during* the chemical reaction is a must.

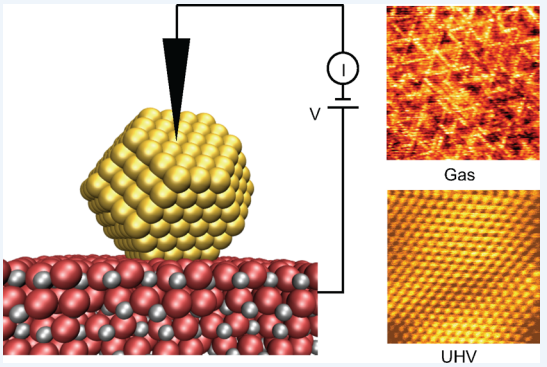

KEY REFERENCES

- Frenken, J. W. M.; Groot, I. M. N. Seeing dynamic phenomena with live scanning tunneling microscopy. *MRS Bull.* **2017**, *42*, 834−841.[1] *Overview of the scanning probe microscopy techniques developed at Leiden University to further our fundamental understanding of heterogeneous catalysis at the (near-)atomic scale.*
- van Spronsen, M. A.; Frenken, J. W. M.; Groot, I. M. N. Observing the oxidation of platinum. *Nat. Commun.* **2017**, *8*, 429.[2] *Exposing the surface of Pt(111) to atmospheric pressures of oxygen at elevated temperatures results in the formation of a platinum surface oxide. This is a structure that is only stable under reaction conditions, stressing the need for in situ observations.*
- Roobol, S. B.; Onderwaater, W. G.; van Spronsen, M. A.; Carlà, F.; Balmes, O.; Navarro, V.; Vendelbo, S.; Kooyman, P. J.; Elkjaer, C. F.; Helveg, S.; Felici, R.; Frenken, J. W. M.; Groot, I. M. N. In situ studies of NO reduction by H-2 over Pt using surface X-ray diffraction and transmission electron microscopy. *Phys. Chem. Chem. Phys.* **2017**, *19*, 8485−8495.[3] *Exposing platinum model catalysts to reaction conditions of NO reduction by H_2 results in surface restructuring and faceting.*
- Jankowski, M.; Saedi, M.; La Porta, F.; Manikas, A. C.; Tsakonas, C.; Cingolani, J. S.; Andersen, M.; de Voogd, J. M.; van Baarle, G. J. C.; Reuter, K.; Galiotis, C.; Renaud, G.; Konovalov, O.; Groot, I. M. N. Real-Time Multiscale

Received: July 19, 2021
Published: November 19, 2021

Monitoring and Tailoring of Graphene Growth on Liquid Copper. *ACS Nano* **2021**, *15*, 9638−9648.[4] *Using real-time observations of growth of graphene on liquid copper, we are able to tailor the growth parameters such that very large single-crystalline graphene sheets can be produced. The growth is determined by an interplay of electrostatic interactions and capillary forces on liquid copper.*

1. INTRODUCTION

Catalysis is a crucial science and technology in our everyday life. Without the use of heterogeneous catalysis, we would not be able to produce most of the chemicals and materials we employ on a daily basis.[5] Furthermore, catalysis will be the driving force behind the transition to a society based on sustainable energy. Using catalysis, the rate of reaction can be increased, and additionally, the reaction can be steered toward the desired products. Even though we have been investigating catalysis for the past century, many catalysts and catalytic processes are still being developed via trial-and-error, instead from rational design. Much of what we currently know about catalysis, has come from studies performed under ultrahigh vacuum instead of under the realistic conditions of industrial catalysis, that is, at or above atmospheric pressures and at high temperatures. The main reason for this discrepancy is the fact that techniques able to obtain microscopic and spectroscopic information needed to understand catalysis are not able to be performed under these conditions. To obtain full understanding of catalysis, we have to know what is happening at the surface of the catalyst, the place where the actual chemical reactions mainly occur. However, most techniques able to investigate the catalyst surface are limited to maximum pressures of 10^{-5} mbar and temperatures of 400 K.[6] Although there are catalytic systems where the results obtained in vacuum are valid under realistic industrial conditions,[7,8] there are also many cases where this "pressure gap" influences the reaction mechanisms.[9−14] Therefore, it is of uncompromising importance to investigate catalysis under more realistic conditions, with the possibility of doing this at the atomic scale. To this end, much progress has been made in the past years to adapt ultrahigh vacuum techniques to conditions of atmospheric pressures. For an overview of these developments, see ref 15.

When one aims to obtain structural information about a catalytic surface at the (near-)atomic scale, traditionally scanning tunneling microscopy (STM) and atomic force microscopy (AFM) have been the methods of choice. These are techniques that are in principle able to obtain atomic resolution under a wide range of conditions: from 10^{-11} mbar to atmospheric pressures, and from very low (millikelvin) to very high temperatures (1000 K).[16] Therefore, scanning probe microscopy is able to obtain information at the atomic scale about the catalytic surface under reaction conditions. Several microscopes have been developed that image the catalyst's surface during the actual chemical reaction and that are suitable to observe changes to the catalyst surface due to the presence of reactants and products.[17−21] The big disadvantage of these microscopy techniques, however, is that they are "chemically blind": they are able to observe atoms at the surface, but it is not clear a priori which atoms. To be able to elucidate the chemical nature of the atoms observed, spectroscopy techniques are the method of choice, for example, polarization-modulation infrared reflection absorption spectroscopy (PM-IRRAS),[22] X-ray photoelectron spectroscopy (XPS),[23] or X-ray absorption spectroscopy.[24,25] However, spectroscopy methods in general do not provide chemical information at the nanoscale, since often a larger area, on the order of micrometers, is probed.

In this Account, I will provide an overview of some of the in situ and operando techniques that we have developed and still are developing at Leiden University, and I will show some examples of scientific insights we have obtained using these techniques.

2. ReactorSTM AND ReactorAFM

2.1. Instrument Design

Over the past two decades, we have developed two novel setups, the so-called ReactorSTM[1,20,26,27] and ReactorAFM.[21,26,27] The designs of these microscopes are fundamentally different from other high-pressure STMs and AFMs. In conventional designs, the entire microscope is contained inside a high-pressure cell,[18,19,28−31] prohibiting employing aggressive chemicals and making simultaneous activity measurements difficult. In our design, however, only the tip or tuning fork holder and the tip or tuning fork are present inside the atmospheric-pressure cell. When designing the microscope, a few requirements had to be taken into account. The first aim was to build a microscope suitable to investigate catalysis under industrial conditions of elevated temperatures and atmospheric pressures, with the capability of obtaining atomic resolution in the STM mode and step resolution in the AFM mode. Second, the imaging of the catalyst surface should be combined with activity measurements using mass spectrometry. To perform operando studies, the time resolution of the mass spectrometer should be less than 10 s. Third, to ensure accurate activity measurements, and to prevent corrosion of vital microscope components, no chemistry should take place elsewhere than on the catalyst surface itself. Last, the setup should enable the preparation of model systems under ultrahigh vacuum conditions. No transfer via air is allowed between preparation and reaction studies under industrial conditions.

To meet these criteria, we make use of the design as shown in Figure 1. The high-pressure cell (reactor) is located in a UHV chamber, to ensure clean preparation of well-defined, highly ordered catalysts. Inlet and outlet gas lines are connected to the high-pressure cell. Gases are administered via home-built gas

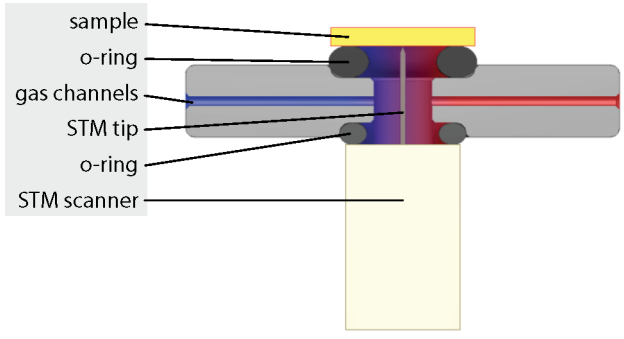

Figure 1. Drawing of the ReactorSTM, showing the concept. Only the STM tip is contained inside the reactor, without exposing the STM scanner to the gases. One side of the reactor is formed by pressing the sample to the Kalrez seal, the other walls are made from Zerodur and therefore are chemically inert. Two seals separate the atmospheric-pressure environment from the surrounding UHV chamber. Reproduced with permission from ref 20. Copyright 2014 American Institute of Physics.

https://doi.org/10.1021/acs.accounts.1c00429
Acc. Chem. Res. 2021, 54, 4334−4341

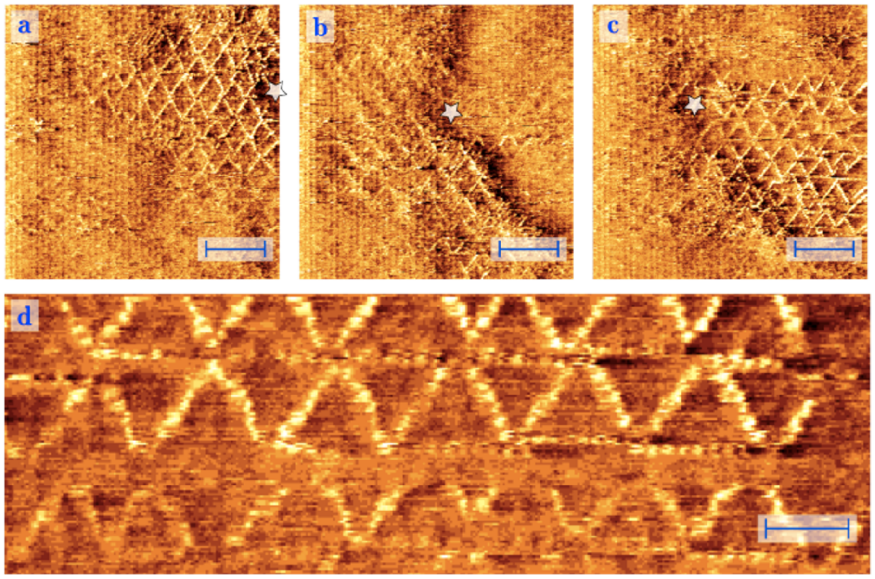

Figure 2. (a–c) Surface oxide with spoked-wheel structure formed on Pt(111) during exposure to 1 bar O_2 at ∼530 K. The star indicates the slowly changing field-of-view due to thermal drift. (d) Enlarged detail displaying atomic resolution in the spokes. Scale bars represent 4 nm (a–c) and 2 nm (d). Reproduced with permission from ref 2. Copyright 2017 Springer Nature.

cabinets[20] and the outlet gases (reactants and products) are analyzed with mass spectrometry.

The only parts of the microscope that are exposed to gases in the reactor are the tip or tuning fork and the tip or tuning fork holder. The high-pressure cell is separated from UHV via two seals: the bottom O-ring (made from Viton) separates the atmospheric-pressure environment from the piezo element (tip actuator), and the top O-ring (made from Kalrez) is located between the sample and the top of the reactor. The catalyst can be heated via radiation from the back side (upper part in Figure 1). Since the Kalrez seal is in direct contact with the sample, and due to its specifications, the maximum operation temperature of the microscope corresponds to 600 K.

Laser deflection techniques are commonly used in AFM to detect the motion of the cantilever. However, in our design no optical access to the tip is possible, since the reactor volume is only 0.05 mL. Therefore, we read out the piezo-electric signal of a quartz tuning fork.[32] Due to its high stiffness, the quartz tuning fork will be relatively insensitive to the presence of the gas-phase reactants and products. The ReactorAFM is operated in the frequency-modulation mode, that is, we make use of non-contact AFM. We oscillate the tuning fork at resonance with an amplitude between 10 pm and 100 nm. When the tip approaches the catalyst surface, the resonance frequency will shift, due to change of the effective spring coefficient of the tuning fork because of tip–sample interactions. We measure the tuning fork's resonance frequency using a phase-locked loop. When investigating the surface, we measure at constant frequency shift. This is done by using the output signal of the phase-locked loop as input for the height feedback loop. Via a separate feedback system, the drive amplitude can be adjusted to keep a constant oscillation amplitude, ensuring that the surface of constant frequency shift corresponds to a surface of constant force gradient. We control the microscopes using fast analog or digital SPM control electronics (Leiden Probe Microscopy B.V.) capable of video-rate STM imaging.[33,34]

The complete setup has three UHV chambers: an XPS chamber, a preparation chamber, and the STM/AFM chamber with the microscope. In the XPS chamber, XPS can be performed under UHV conditions. In addition, a sample library is present for extra sample and the chamber consists of a sample load-lock. In the preparation chamber, single crystals can be cleaned using argon ion sputtering. To prepare more complex model catalysts with metallic or oxidic nanoparticles, an electron-beam evaporator is present. Furthermore, samples can be characterized using LEED and AES.

2.2. Oxidation of Pt(111)

Platinum is one of the components of the automotive catalyst that neutralizes toxic emissions, for example, catalyzing the oxidation of carbon monoxide to carbon dioxide and the oxidation of hydrocarbons to carbon dioxide and water. Despite many years of research, the active phase of platinum during oxidation reactions remained uncertain. Using surface X-ray diffraction (SXRD) under reaction conditions, the formation of α-PtO_2 was observed.[35,36] Theoretical ab initio thermodynamics studies confirmed that under the experimental conditions used, this should indeed be the most stable phase.[37,38] However, near-ambient-pressure X-ray photoelectron spectroscopy (NAP-XPS) studies performed at similar temperatures as the SXRD studies but, due to the technical limitations of the experiments, at lower pressures, observed the formation of a surface oxide. Only at much higher temperatures a bulk oxide was formed.[39]

To shed light on this discrepancy between SXRD and NAP-XPS, we investigated the oxidation of Pt(111) using our ReactorSTM.[2] We exposed the surface to O_2 pressures between 1 and 5 bar at temperatures between 300 and 538 K. We observed different surface structures, depending on pressure and temperature, but none of them could be attributed to α-PtO_2.

When exposing Pt(111) to 1 bar of O_2 at ∼530 K, we observed the appearance of triangular features that assembled into spoked-wheel superstructures over time, see Figure 2. The average edge length is 2.2 ± 0.1 nm, corresponding to 7.9 ± 0.4 Pt(111) lattice constants. From the atomic-resolution images in Figure 2c,d, we measured the atomic periodicity in the rows to be 0.30 ± 0.01 nm, significantly larger than the lattice constant of Pt(111) (0.278 nm), but close to that of the surface oxides observed under UHV conditions,[40] α-PtO_2[41] and PtO.[42]

https://doi.org/10.1021/acs.accounts.1c00429
Acc. Chem. Res. 2021, 54, 4334–4341

Therefore, we consider this structure as a surface oxide containing 1D oxide rows. Each oxide row consists of 8 Pt atoms, with 7 Pt atoms in the layer below. The top Pt atoms of the spoked-wheel structure are not on top of the surface, but are slightly lifted within the top layer. The O coverage of this proposed structure is 0.75 ML, three times more than the maximum coverage obtained in UHV.[43,44] The structure observed here was never observed before nor predicted by theory.

Simultaneously with the formation of the spoked-wheel structure, the platinum surface became rough, see Figure 3. The

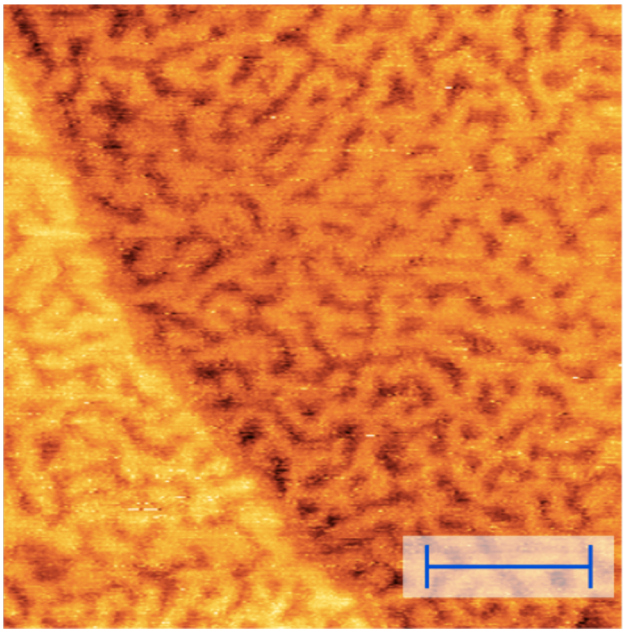

Figure 3. Large-scale image of the surface oxide after 43 min at 1 bar O_2 and ~530 K. Scale bar represents 20 nm. Reproduced with permission from ref 2. Copyright 2017 Springer Nature.

observed structure shows a complicated network of worm-like islands. The depth between the islands was measured as 0.21 ± 0.02 nm, corresponding to the platinum step height. We conclude that a flat terrace of platinum upon high-pressure O_2 exposure transformed into networks of monatomic-high, worm-shaped islands. The observed large-scale roughening is induced by the stress the oxide exerts on the surface, and has been observed before when exposing Pt(111) to CO oxidation conditions in an oxygen-rich flow.[45]

Under higher pressures, starting from 2.2 bar O_2, we observed a new surface structure, see Figure 4. This structure consists of parallel rows. The row-to-row distance corresponds to 0.46 ± 0.01 nm, which is close to $\sqrt{3} \times a$, where a is the nearest-neighbor Pt distance. Therefore, this observed structure is commensurate with Pt(111). The O coverage in this surface oxide corresponds to 0.88 ML. We observed two types of this row structure: one where the rows are "in phase", minimizing the O−O separation between adjacent stripes, and expected for attractive O−O interactions, and one where the rows are "out-of-phase", maximizing the O−O separation, and expected for repulsive interactions. This results in a (2×8) and a (4×8) unit cell, respectively. After evacuation of the reactor and cooling down to room temperature, both observed structures were no longer visible, indicating that these structures are only stable under reaction conditions.

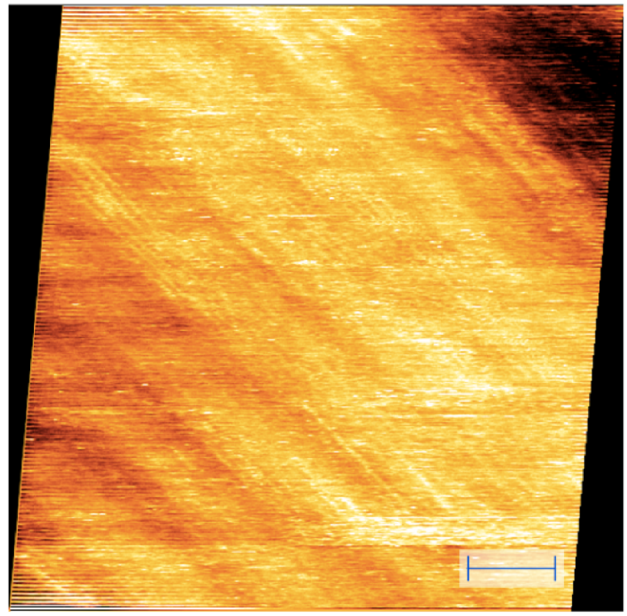

Figure 4. Row structure formed at pressures above 2.2 bar O_2. Scale bar represents 4 nm. Reproduced with permission from ref 2. Copyright 2017 Springer Nature.

3. OPERANDO SURFACE X-RAY DIFFRACTION

X-ray-based techniques are very suitable to use under atmospheric-pressure conditions, due to the weak interaction of X-rays with gases. Therefore, the surfaces of catalysts have been investigated under reaction conditions using surface X-ray diffraction (SXRD)[46,47] and grazing-incidence small-angle X-ray scattering (GISAXS).[48] Typically, an SXRD-type reactor consists of a chamber with X-ray-transparent walls (aluminum or beryllium) into which gases can be introduced. For preparation of atomically clean surfaces, these reactors need to contain typical UHV equipment such as an ion sputter gun. This requirement results in large reactor volumes (often >1 L), and hence, operation in batch mode only. Even though results for batch reactors suffer from changes in gas composition over time, meaningful insights have been obtained for these setups.[13,49]

In collaboration with the European Synchrotron Radiation Facility (ESRF), a flow reactor setup has been developed,[50] combining a flow reactor with a UHV environment for sample preparation. Simultaneous structure (via SXRD and GISAXS) and activity (via mass spectrometry) measurements under reaction conditions can be performed.

In the design of the ReactorSXRD setup (see Figure 5), the sample is fixed, to avoid sample realignment with respect to the X-ray beam after preparation. Instead, the upper part of the instrument moves around the sample. The setup consists of two parts connected by a bellow. The upper part (UHV) contains the ion sputter gun and an evaporator for physical vapor deposition of metals. The lower part (reactor) contains the sample. If the bellow is completely extended (see Figure 5a), the instrument is in the configuration for sample preparation under UHV conditions. When the top part is lowered over the sample (see Figure 5b), the small volume around the sample is separated from UHV and can be filled with gases up to 1 bar. The upper part of the reactor consists of a beryllium dome, transparent for X-rays. The gas inlet and outlet lines are mounted below the sample holder support. Gas analysis is performed by leaking some gas into the UHV part of the system, where a mass

https://doi.org/10.1021/acs.accounts.1c00429
Acc. Chem. Res. 2021, 54, 4334−4341

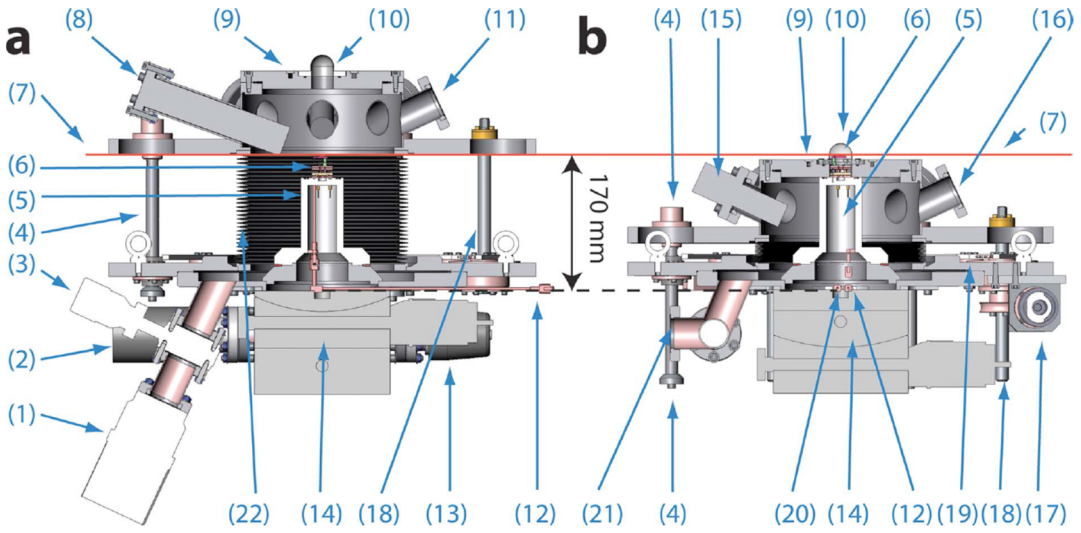

Figure 5. (a) Cut view of the setup in the UHV sample preparation geometry. (b) Cut view of the setup with closed reactor, 90° rotated with respect to the view of panel a. The beam is located 170 mm above the diffractometer sample stage surface. The labels denote (1) turbo pump, (2) mass spectrometer, (3) manual UHV valve, (4) guiding rods for vertical movement of top part of chamber, (5) sample holder foot, (6) sample holder, (7) X-ray beam height, (8) evaporator port, (9) water-cooled top flange, (10) beryllium dome, (11) ion gun port, (12) reactor gas exhaust line, (13) UHV leak valve, (14) Huber five-axis positioning system, (15) cold cathode pressure gauge, (16) blind flange, (17) electromotor and drive shaft, (18) threaded drive rods for vertical movement of top part of chamber, (19) chain drive mechanism for vertical movement, (20) gas entry line, (21) UHV vent valve, and (22) steel bellow. Reproduced with permission from ref 50. Copyright 2010 American Institute of Physics.

spectrometer is located. The sample is heated by a pyrolytic boron nitride heater.

3.1. NO Reduction on Pt(110)

One of the other reactions taking place in automotive catalysis is the reduction of harmful NO, either by H_2 or CO. Here I will discuss the results we obtained for NO reduction by hydrogen on Pt(110) using SXRD.[3] Depending on the reaction conditions, we have observed several surface structures of Pt(110). These observations were confirmed using STM.[51] The observed Pt(110) surface structures consist of two different types: surface reconstructions, which require small rearrangements of Pt atoms, and surface faceting, which requires large transport of Pt atoms. Depending on the partial pressures of NO and H_2 at 1 bar and temperatures between 573 and 673 K, we observed several surface reconstructions, most of them never observed before under UHV conditions. Figure 6 shows an overview of these reconstructions. One of the reconstructions, the (1 × 3) missing-row structure observed in H_2, probably corresponds to the one also observed in vacuum on the clean sample and similar to the structure observed by Robinson et al.[52] The fact that under ambient-pressure conditions reconstructions are found that are not observed in UHV can be explained by the higher mobility of Pt atoms at atmospheric pressure and the adsorption of species on the surface that may form different adsorbate structures under reaction conditions. Other surface structures we observed are an unstable incommensurate (4 × 3) structure that changed over time into a commensurate one and the stable incommensurate "0.22" surface structure.

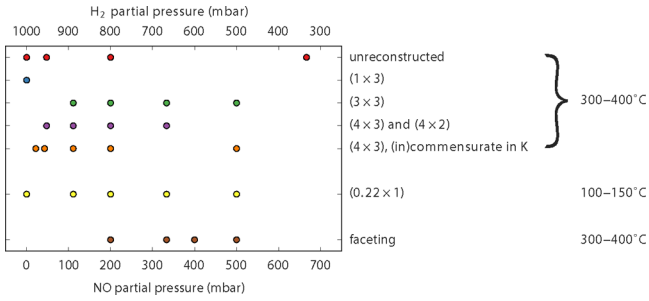

Figure 6. Reconstruction on Pt(110) as a function of NO and H_2 gas composition at 1 bar. The catalyst temperature was between 573 and 673 K, except for the "0.22" reconstruction, which we observed at ∼373−423 K. Reproduced with permission from ref 3. Copyright 2017 Royal Society of Chemistry.

At the end of the exposure of Pt(110) to the NO reduction reaction, under conditions that we probed earlier, the surface started faceting. These facets are tilted by 8−12° away from the (110) surface in the [$\bar{1}$10] direction. With more NO present smaller tilt angles were observed. After ∼4 h, the system reached steady state, indicating that the facets were growing in average size. The observed tilt angle around 10° suggests a surface structure of (320), a crystal plane making an angle of 11.3° with the (110) plane. We also observed indications of the presence of (430) and (540) orientations, especially at higher NO pressure. The surface faceting under high-pressure conditions could be caused by strong binding of adsorbates to the step edges,[53,54] where NO, H_2O, NH_3, or O are likely candidates as observed from our mass spectrometry data or by adsorbate-induced stress[55,56] due to the strong repulsive interactions between NO molecules at higher coverages.

4. COMBINING SCANNING TUNNELING MICROSCOPY WITH X-RAYS

Even though STM/AFM and SXRD are very powerful techniques to investigate catalysis under reaction conditions, both have their respective serious drawbacks. For STM/AFM, this is the fact that the techniques are able to provide atomic-scale structural information but they are "chemically blind": we observe the atoms on the surface but cannot know a priori which atoms they are. For SXRD, this is the fact that the X-ray beam spot is large, and therefore only average information can be obtained. Ideally, one would be able to obtain chemical

https://doi.org/10.1021/acs.accounts.1c00429
Acc. Chem. Res. 2021, 54, 4334−4341

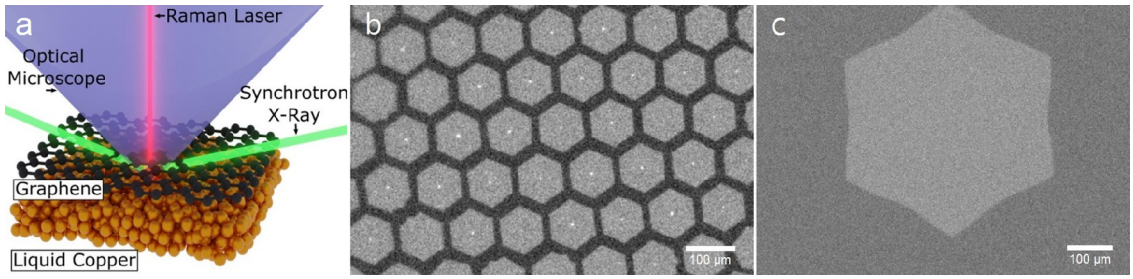

Figure 7. (a) Configuration of in situ monitoring methods applied to a graphene layer grown on liquid copper. (b) Example of in situ radiation-mode optical microscopy of self-organized hexagonal graphene flakes on liquid copper. (c) One single-crystal flake grown to millimeter size.

information on the atomic scale. By combination of STM with X-rays, whereby the STM tip is used as a detector collecting the current, it is possible to obtain local X-ray absorption spectra, with roughly 2 nm resolution.[57−59] Under vacuum conditions, until recently the only known studies, the electrons collected by the STM tip have three different origins: the photoelectron current, the regular tunneling current (topography), and an increase of the tunneling current induced by the X-rays. Those latter electrons are the ones providing local X-ray absorption information.

To be able to obtain this local chemical information under reaction conditions (i.e., atmospheric pressures and elevated temperatures), two major challenges need to be overcome: Due to the gas pressure, prohibitively large ion currents are generated, and due to elevated temperatures, and therefore thermal drift, fast response in the height feedback is necessary. In my group, we have been able to overcome these challenges, by making use of an electronics scheme to separate the X-ray-induced and the topographic ("normal") tunneling current, and by making use of coaxially shielded STM tips[58] and a mounting configuration that effectively suppresses the ion current background.[60] Using a previously developed STM/AFM that can be mounted on top of our SXRD chamber,[61] we have been able to measure the local, X-ray-induced tunneling current of Au(111) in a gas environment of 800 mbar at room temperature.[60] The next steps will be to further optimize the technique to be able to measure local X-ray absorption spectra at elevated temperatures during a chemical reaction (i.e., in the presence of multiple reactants).

5. IN SITU REACTOR FOR GRAPHENE GROWTH ON LIQUID COPPER

To be able to make use of graphene and other two-dimensional (2D) materials in industrial applications, reproducible mass production of large and defect-free specimens is needed. Currently, the method mostly used for the production of graphene is chemical vapor deposition (CVD) of methane on solid copper at high temperatures.[62] Nucleation of the C-species happens at random places, resulting in layers of graphene with many domains and defects.

Recently, it was found that liquid metal catalysts (LMCats) can be employed to grow graphene and other 2D materials faster and with significantly higher quality.[63] When the 2D material is grown on an atomically flat isotropic melt such as the liquid metal surface, the underlying structure of the catalyst has less influence on the 2D material's quality. Since the growth process is influenced by many parameters such as pressure, temperature, gas flow, and partial pressure, optimizing the CVD process has mainly led to empirical recipes. A real understanding of the growth process, which has a stochastic nature, has not been obtained yet.

To be able to follow the growth process of graphene on liquid copper in situ and in real time, we have developed and implemented a reactor in which we are able to monitor this at multiple time and length scales using Raman spectroscopy, optical microscopy, grazing-incidence X-ray diffraction, and X-ray reflectivity.[4,64] The LMCat reactor, located at ESRF-ID10, enables us to tailor the quality, crystal shape, and crystal size (see Figure 7a). Using radiation-mode optical microscopy, we observed the growth morphology and the kinetics at micrometer-scale in real time. With in situ Raman spectroscopy, we confirmed the graphene to be monolayer and we obtained information about crystallinity and defects. At the atomic scale, we were able to measure the lattice constant and the corrugation of the graphene sheets using grazing-incidence X-ray diffraction. Employing synchrotron X-ray reflectivity, we determined the roughness of graphene, the number of layers, and the gap between liquid copper and graphene. To obtain further understanding of our experiments, we used multiscale simulations.[4,65]

Using our in situ monitoring capabilities, we investigated different CVD growth processes. First, we studied the growth of graphene by injecting a short pulse of methane at high partial pressure. Many flakes are produced that first grow in size and then form a 2D hexagonal network, governed by an interplay between electrostatic interactions (short-range) and capillary forces (long-range) (see Figure 7b). Simulations confirmed the formation of such a superordered assembly. On a solid surface, graphene flakes are immobile and spontaneous ordering is not observed. Finally, the flakes merge to form a continuous sheet; however, due to slight misorientations between neighboring flakes upon coalescence, some domain boundaries remain in the sheet. Therefore, we used the possibility of feedback-control that our setup offers to reduce the defects in the graphene sheet. Hereby, we were able to tailor the parameters such that nucleation of only a single flake that grew to millimeter size occurred (see Figure 7c). The Raman and X-ray reflectivity spectra of our graphene grown on liquid copper compare favorably to those of exfoliated graphene.[4]

6. CONCLUSIONS AND OUTLOOK

Using the in situ/operando setups developed in our group, we are able to obtain direct structural information about the catalyst surface in combination with its performance while the chemical reaction is taking place. From the examples shown here and also found from other systems we study, it is clear that in many cases there is a discrepancy between the surface structure present under reaction conditions and the structure present under UHV conditions. This makes it clear that to be able to obtain a full

https://doi.org/10.1021/acs.accounts.1c00429
Acc. Chem. Res. 2021, 54, 4334−4341

fundamental understanding of heterogeneous catalysis, catalysts have to be studied during the actual reaction, making use of advanced high-pressure techniques such as those described in this work. To further advance these studies, we are currently designing a combined AFM-STM setup for catalytic studies, based on the design of the ReactorSTM[20] and the Reactor-AFM.[21] Furthermore, we are developing a new ReactorSTM that will be able to measure at temperatures up to 1200 K. The next step, which we are already taking, is the investigation of more complex catalysts, such as metallic, oxidic, or sulfidic nanoparticles on a support, instead of single-crystal surfaces only, thereby bridging the materials gap as well.

AUTHOR INFORMATION

Corresponding Author

Irene M. N. Groot − *Leiden Institute of Chemistry, Leiden University, 2300 RA Leiden, the Netherlands;* orcid.org/0000-0001-9747-3522; Phone: +31 71 5277361; Email: i.m.n.groot@lic.leidenuniv.nl

Complete contact information is available at: https://pubs.acs.org/10.1021/acs.accounts.1c00429

Notes

The author declares no competing financial interest.

Biography

During her Ph.D. studies at Leiden University, **Irene Groot** studied hydrogen dissociation on metal surfaces, using supersonic molecular beams and density functional theory and quantum dynamics calculations. She then moved to the Fritz Haber Institute where she investigated CO oxidation using scanning tunneling microscopy. With a personal Veni fellowship from the Dutch Research Council (NWO), Groot moved to the Leiden Institute of Physics. Here she investigated chlorine production under reaction conditions, using scanning tunneling microscopy, followed by starting her own group. In 2015, this group was moved to the Leiden Institute of Chemistry, where currently Groot has a tenured associate professor position. Her research focuses on the structure−activity relationships of catalysts under realistic conditions, using different operando techniques such as scanning probe microscopy and synchrotron-X-ray-based methods. To this end, Groot is also developing equipment for high-pressure surface science and operando catalysis research. Current topics being investigated are hydrodesulfurization, Fischer−Tropsch synthesis, methanol steam reforming, automotive catalysis, chlorine production, two-dimensional materials, and graphene growth on liquid copper.

ACKNOWLEDGMENTS

I would like to thank all past and current Ph.D. students, postdoctoral fellows, and research engineers of the Groot and Frenken groups at Leiden University for their contributions to this research endeavor. Funding from the Dutch Research Council (NWO), grant 016.Vidi.189.022, is acknowledged.

REFERENCES

(1) Frenken, J. W. M.; Groot, I. M. N. Seeing dynamic phenomena with live scanning tunneling microscopy. *MRS Bull.* **2017**, *42*, 834−841.
(2) van Spronsen, M. A.; Frenken, J. W. M.; Groot, I. M. N. Observing the oxidation of platinum. *Nat. Commun.* **2017**, *8*, 429.
(3) Roobol, S. B.; Onderwaater, W. G.; van Spronsen, M. A.; Carlà, F.; Balmes, O.; Navarro, V.; Vendelbo, S.; Kooyman, P. J.; Elkjaer, C. F.; Helveg, S.; Felici, R.; Frenken, J. W. M.; Groot, I. M. N. In situ studies of NO reduction by H-2 over Pt using surface X-ray diffraction and transmission electron microscopy. *Phys. Chem. Chem. Phys.* **2017**, *19*, 8485−8495.
(4) Jankowski, M.; Saedi, M.; La Porta, F.; Manikas, A. C.; Tsakonas, C.; Cingolani, J. S.; Andersen, M.; de Voogd, J. M.; van Baarle, G. J. C.; Reuter, K.; Galiotis, C.; Renaud, G.; Konovalov, O.; Groot, I. M. N. Real-Time Multiscale Monitoring and Tailoring of Graphene Growth on Liquid Copper. *ACS Nano* **2021**, *15*, 9638−9648.
(5) Thomas, J.; Thomas, W. *Principles and Practice of Heterogeneous Catalysis*, 2nd Ed.; Wiley-VCH: Weinheim, 2015.
(6) Wintterlin, J. Scanning tunneling microscopy studies of catalytic reactions. *Adv. Catal.* **2000**, *45*, 131−206.
(7) Ertl, G. Primary steps in catalytic synthesis of ammonia. *J. Vac. Sci. Technol., A* **1983**, *1*, 1247−1253.
(8) Rodriguez, J. A.; Goodman, D. W. High-pressure catalytic reactions over single-crystal metal surfaces. *Surf. Sci. Rep.* **1991**, *14*, 1−107.
(9) Su, X.; Cremer, P. S.; Shen, Y. R.; Somorjai, G. A. High-pressure CO oxidation on Pt(111) monitored with infrared-visible sum frequency generation (SFG). *J. Am. Chem. Soc.* **1997**, *119*, 3994−4000.
(10) Over, H.; Kim, Y. D.; Seitsonen, A. P.; Wendt, S.; Lundgren, E.; Schmid, M.; Varga, P.; Morgante, A.; Ertl, G. Atomic-scale structure and catalytic reactivity of the RuO2(110) surface. *Science* **2000**, *287*, 1474−1476.
(11) Hendriksen, B. L. M.; Frenken, J. W. M. CO oxidation on Pt(110): Scanning tunneling microscopy inside a high-pressure flow reactor. *Phys. Rev. Lett.* **2002**, *89*, 046101.
(12) Over, H.; Muhler, M. Catalytic CO oxidation over ruthenium - bridging the pressure gap. *Prog. Surf. Sci.* **2003**, *72*, 3−17.
(13) Ackermann, M. D.; Pedersen, T. M.; Hendriksen, B. L. M.; Robach, O.; Bobaru, S. C.; Popa, I.; Quirós, C.; Kim, H.; Hammer, B.; Ferrer, S.; Frenken, J. W. M. Structure and reactivity of surface oxides on Pt(110) during catalytic CO oxidation. *Phys. Rev. Lett.* **2005**, *95*, 25505.
(14) Westerström, R.; Gustafson, J.; Resta, A.; Mikkelsen, A.; Andersen, J. N.; Lundgren, E.; Seriani, N.; Mittendorfer, F.; Schmid, M.; Klikovits, J.; Varga, P.; Ackermann, M. D.; Frenken, J. W. M.; Kasper, N.; Stierle, A. Oxidation of Pd(553): From ultrahigh vacuum to atmospheric pressure. *Phys. Rev. B: Condens. Matter Mater. Phys.* **2007**, *76*, 155410.
(15) Frenken, J. W. M.; Groot, I. M. N. *Operando Research in Heterogeneous Catalysis*; Springer Verlag, 2017.
(16) Chen, C. J. *Introduction to Scanning Tunneling Microscopy*; Oxford University Press, 1993.
(17) Weeks, B. L.; Durkan, C.; Kuramochi, H.; Welland, M. E.; Rayment, T. A high pressure, high temperature, scanning tunneling microscope for in situ studies of catalysts. *Rev. Sci. Instrum.* **2000**, *71*, 3777−3781.
(18) Rössler, M.; Geng, P.; Wintterlin, J. A high-pressure scanning tunneling microscope for studying heterogeneous catalysis. *Rev. Sci. Instrum.* **2005**, *76*, 023705.
(19) Tao, F.; Tang, D.; Salmeron, M.; Somorjai, G. A. A new scanning tunneling microscope reactor used for high-pressure and high-temperature catalysis studies. *Rev. Sci. Instrum.* **2008**, *79*, 084101.
(20) Herbschleb, C. T.; et al. The ReactorSTM: Atomically resolved scanning tunneling microscopy under high-pressure, high-temperature catalytic reaction conditions. *Rev. Sci. Instrum.* **2014**, *85*, 083703.
(21) Roobol, S. B.; Cañas-Ventura, M. E.; Bergman, M.; van Spronsen, M. A.; Onderwaater, W. G.; van der Tuijn, P. C.; Koehler, R.; Ofitserov, A.; van Baarle, G. J. C.; Frenken, J. W. M. The ReactorAFM: Non-contact atomic force microscope operating under high-pressure and high-temperature catalytic conditions. *Rev. Sci. Instrum.* **2015**, *86*, 033706.
(22) Beitel, G. A.; Laskov, A.; Oosterbeek, H.; Kuipers, E. W. Polarization modulation infrared reflection absorption spectroscopy of CO adsorption on Co(0001) under a high-pressure regime. *J. Phys. Chem.* **1996**, *100*, 12494−12502.
(23) Salmeron, M.; Schlögl, R. Ambient pressure photoelectron spectroscopy: A new tool for surface science and nanotechnology. *Surf. Sci. Rep.* **2008**, *63*, 169−199.

(24) Knop-Gericke, A.; Hävecker, M.; Schedel-Niedrig, T.; Schlögl, R. Probing the electronic structure of an active catalyst surface under high-pressure reaction conditions: the oxidation of methanol over copper. *Catal. Lett.* **2000**, *66*, 215−220.
(25) Evans, J.; Puig-Molina, A.; Tromp, M. In situ EXAFS characterization of nanoparticulate catalysts. *MRS Bull.* **2007**, *32*, 1038−1043.
(26) Frenken, J. W. M.; Groot, I. M. N. In *Operando Research in Heterogeneous Catalysis*; Frenken, J. W. M., Groot, I. M. N., Eds.; Springer Verlag, 2017; Chapter 1.
(27) Groot, I. M. N. In *Encyclopedia of Interfacial Chemistry: Surface Science and Electrochemistry*; Wandelt, K., Ed.; Elsevier, 2018; Vol. *1*; p 336.
(28) Laegsgaard, E.; Österlund, L.; Thostrup, P.; Rasmussen, P. B.; Stensgaard, I.; Besenbacher, F. A high-pressure scanning tunneling microscope. *Rev. Sci. Instrum.* **2001**, *72*, 3537−3542.
(29) Kolmakov, A.; Goodman, D. W. In situ scanning tunneling microscopy of individual supported metal clusters at reactive gas pressures from 10(−8) to 10(4) Pa. *Rev. Sci. Instrum.* **2003**, *74*, 2444−2450.
(30) Lievonen, J.; Ranttila, K.; Ahlskog, M. Environmental chamber for an atomic force microscope. *Rev. Sci. Instrum.* **2007**, *78*, 043703.
(31) D'Agostino, D.; Jay, D.; McNally, H. Development and testing of hyperbaric atomic force microscopy (AFM) for biological applications. *Microsc. Microanal.* **2010**, *16*, 1042−1043.
(32) Giessibl, F. J.; Hembacher, S.; Bielefeldt, H.; Mannhart, J. Subatomic features on the silicon (111)-(7 × 7) surface observed by atomic force microscopy. *Science* **2000**, *289*, 422−425.
(33) Rost, M.; et al. Scanning probe microscopes go video rate and beyond. *Rev. Sci. Instrum.* **2005**, *76*, 053710.
(34) Rost, M. J.; van Baarle, G. J. C.; Katan, A. J.; van Spengen, W. M.; Schakel, P.; van Loo, W. A.; Oosterkamp, T. H.; Frenken, J. W. M. Video-rate scanning probe control challenges: setting the stage for a microscopy revolution. *Asian Journal of Control* **2009**, *11*, 110−129.
(35) Ackermann, M. D. Operando SXRD: A New View on Catalysis. Ph.D. Thesis, Leiden University, 2007.
(36) Ellinger, C.; Stierle, A.; Robinson, I. K.; Nefedov, A.; Dosch, H. Atmospheric pressure oxidation of Pt(111). *J. Phys.: Condens. Matter* **2008**, *20*, 184013.
(37) Seriani, N.; Mittendorfer, F. Platinum-group and noble metals under oxidizing conditions. *J. Phys.: Condens. Matter* **2008**, *20*, 184023.
(38) Zhu, T.; Sun, S. G.; van Santen, R. A.; Hensen, E. J. M. Reconstruction of Clean and Oxygen-Covered Pt(110) Surfaces. *J. Phys. Chem. C* **2013**, *117*, 11251−11257.
(39) Miller, D. J.; Oberg, H.; Kaya, S.; Sanchez Casalongue, H.; Friebel, D.; Anniyev, T.; Ogasawara, H.; Bluhm, H.; Pettersson, L. G. M.; Nilsson, A. Oxidation of Pt(111) under Near-Ambient Conditions. *Phys. Rev. Lett.* **2011**, *107*, 195502.
(40) Devarajan, S. P.; Hinojosa, J. A., Jr.; Weaver, J. F. STM study of high-coverage structures of atomic oxygen on Pt(111): p(2 × 1) and Pt oxide chain structures. *Surf. Sci.* **2008**, *602*, 3116−3124.
(41) Galloni, E. E.; Busch, R. H. The structure of platinum oxides. *J. Chem. Phys.* **1952**, *20*, 198−199.
(42) Westwood, W. D.; Bennewitz, D. Formation of PtO films by reactive sputtering. *J. Appl. Phys.* **1974**, *45*, 2313−2316.
(43) Gland, J. L. Molecular and atomic adsorption of oxygen on the Pt(111) and Pt(S)-12(111)x(111) surfaces. *Surf. Sci.* **1980**, *93*, 487−514.
(44) Materer, N.; Starke, U.; Barbieri, A.; Doll, R.; Heinz, K.; van Hove, M. A.; Somorjai, G. A. Reliability of detailed LEED structural analyses - Pt(111) and Pt(111)-p(2 × 2)-O. *Surf. Sci.* **1995**, *325*, 207−222.
(45) Bobaru, S. C. High-Pressure STM studies of Oxidation Catalysis. Ph.D. Thesis, Leiden University, 2006.
(46) Robinson, I. K.; Tweet, D. J. Surface X-ray diffraction. *Rep. Prog. Phys.* **1992**, *55*, 599−651.
(47) Feidenhans'l, R. Surface-structure determination by X-ray diffraction. *Surf. Sci. Rep.* **1989**, *10*, 105−188.
(48) Renaud, G.; Lazzari, R.; Leroy, F. Probing surface and interface morphology with Grazing Incidence Small Angle X-Ray Scattering. *Surf. Sci. Rep.* **2009**, *64*, 255−380.
(49) Over, H.; Balmes, O.; Lundgren, E. Direct comparison of the reactivity of the non-oxidic phase of Ru(0001) and the RuO2 phase in the CO oxidation reaction. *Surf. Sci.* **2009**, *603*, 298−303.
(50) van Rijn, R.; Ackermann, M. D.; Balmes, O.; Dufrane, T.; Geluk, A.; Gonzalez, H.; Isern, H.; de Kuyper, E.; Petit, L.; Sole, V. A.; Wermeille, D.; Felici, R.; Frenken, J. W. M. Ultrahigh vacuum/high-pressure flow reactor for surface x-ray diffraction and grazing incidence small angle x-ray scattering studies close to conditions for industrial catalysis. *Rev. Sci. Instrum.* **2010**, *81*, 014101.
(51) van Spronsen, M. A.; van Baarle, G. J. C.; Herbschleb, C. T.; Frenken, J. W. M.; Groot, I. M. N. High-pressure operando STM studies giving insight in CO oxidation and NO reduction over Pt(110). *Catal. Today* **2015**, *244*, 85−95.
(52) Robinson, I. K.; Eng, P. J.; Romainczyk, C.; Kern, K. X-ray determination of the 1 × 3 reconstruction of Pt(110). *Phys. Rev. B: Condens. Matter Mater. Phys.* **1993**, *47*, 10700−10705.
(53) Thostrup, P.; Christoffersen, E.; Lorensen, H. T.; Jacobsen, K. W.; Besenbacher, F.; Norskov, J. K. Adsorption-induced step formation. *Phys. Rev. Lett.* **2001**, *87*, 126102.
(54) Hammer, B. The NO plus CO reaction catalyzed by flat, stepped, and edged Pd surfaces. *J. Catal.* **2001**, *199*, 171−176.
(55) Hanesch, P.; Bertel, E. Mesoscopic self-organization induced by intrinsic surface stress on Pt(110). *Phys. Rev. Lett.* **1997**, *79*, 1523−1526.
(56) Grossmann, A.; Erley, W.; Ibach, H. Adsorbate-induced surface stress - CO on Ni(100) and Ni(111). *Surf. Sci.* **1994**, *313*, 209−214.
(57) Saito, A.; et al. Development of a scanning tunneling microscope for in situ experiments with a synchrotron radiation hard-X-ray microbeam. *J. Synchrotron Radiat.* **2006**, *13*, 216−220.
(58) Shirato, N.; Cummings, M.; Kersell, H.; Li, Y.; Stripe, B.; Rosenmann, D.; Hla, S.; Rose, V. Elemental Fingerprinting of Materials with Sensitivity at the Atomic Limit. *Nano Lett.* **2014**, *14*, 6499−6504.
(59) Okuda, T.; Eguchi, T.; Akiyama, K.; Harasawa, A.; Kinoshita, T.; Hasegawa, Y.; Kawamori, M.; Haruyama, Y.; Matsui, S. Nanoscale Chemical Imaging by Scanning Tunneling Microscopy Assisted by Synchrotron Radiation. *Phys. Rev. Lett.* **2009**, *102*, 105503.
(60) Mom, R. V.; et al. Simultaneous scanning tunneling microscopy and synchrotron X-ray measurements in a gas environment. *Ultramicroscopy* **2017**, *182*, 233−242.
(61) Onderwaater, W. G.; van der Tuijn, P. C.; Mom, R. V.; van Spronsen, M. A.; Roobol, S. B.; Saedi, A.; Drnec, J.; Isern, H.; Carlà, F.; Dufrane, T.; Koehler, R.; Crama, B.; Groot, I. M. N.; Felici, F.; Frenken, J. W. M. Combined scanning probe microscopy and x-ray scattering instrument for in situ catalysis investigations. *Rev. Sci. Instrum.* **2016**, *87*, 113705.
(62) Mattevi, C.; Kim, H.; Chhowalla, M. A review of chemical vapour deposition of graphene on copper. *J. Mater. Chem.* **2011**, *21*, 3324−3334.
(63) Tsakonas, C.; Dimitropoulos, M.; Manikas, A. C.; Galiotis, C. Growth and in situ characterization of 2D materials by chemical vapour deposition on liquid metal catalysts: a review. *Nanoscale* **2021**, *13*, 3346−3373.
(64) Saedi, M.; de Voogd, J. M.; Sjardin, A.; Manikas, A. C.; Galiotis, C.; Jankowski, M.; Renaud, G.; La Porta, F.; Konovalov, O.; van Baarle, G. J. C.; Groot, I. M. N. Development of a reactor for the in situ monitoring of 2D materials growth on liquid metal catalysts, using synchrotron x-ray scattering, Raman spectroscopy, and optical microscopy. *Rev. Sci. Instrum.* **2020**, *91*, 013907.
(65) Cingolani, J. S.; Deimel, M.; Kocher, S.; Scheurer, C.; Reuter, K.; Andersen, M. Interface between graphene and liquid Cu from molecular dynamics simulations. *J. Chem. Phys.* **2020**, *153*, 074702.

https://doi.org/10.1021/acs.accounts.1c00429
Acc. Chem. Res. 2021, 54, 4334−4341